DETECTION OF HAIRLINE MANDIBULAR FRACTURE USING MAX-FLOW MIN-CUT AND KOLMOGOROV-SMIRNOV DISTANCE

Ananda S. Chowdhury,[⋆] *Suchendra M. Bhandarkar,*[†] *Robert W. Robinson,*[†] *Jack C. Yu*[⋆†]

E-mails: ananda.chowdhury@gmail.com, suchi@cs.uga.edu, rwr@cs.uga.edu, jyu@mcg.edu

[⋆] Department of Electronics and Telecom. Engg.
Jadavpur University, Calcutta - 700032, India.
[†] Department of Computer Science.
University of Georgia, Athens, GA - 30602, USA.
[⋆†] Department of Plastic Surgery.
Medical College of Georgia, Augusta, GA - 30912, USA.

ABSTRACT

The paper addresses a clinically challenging problem of hairline mandibular fracture detection from Computed Tomography (CT) images. A hairline fracture that has critical clinical importance, can be easily missed due to lack of sharp discontinuity and presence of intensity inhomogeneity, if not scrutinized carefully. In this work, 2D image slices containing mandibles with hairline fractures are separated first from input image sequences of broken craniofacial skeletons. This is achieved through an intensity-based image retrieval scheme with Kolmogorov-Smirnov distance as the measure of similarity and an unbroken mandible as the reference image. Since, a hairline fracture is essentially a discontinuity in the bone contour, we model it as a minimum cut in an appropriately weighted flow network. Existing graph cut-based segmentation framework is enhanced with a novel construction of the flow network, guided by the geometry of the mandible. Ford-Fulkerson algorithm is employed next to obtain a minimum cut, which represents the hairline fracture in these already separated slices. Experimental results demonstrate the effectiveness of the proposed method.

***Index Terms*—** Hairline mandibular fracture, Max-flow min-cut, Kolmogorov-Smirnov distance.

1. INTRODUCTION

Mandibular fractures occur frequently due to gunshot wounds, motor vehicle accidents, sports-related and battlefield-related injuries [1]. The mandible is usually less protected and hence more vulnerable than other parts of the human anatomy, even with full-body armor. The term *hairline fracture* refers to situations where the broken bone fragments are not visibly out of alignment and have incurred very little relative displacement. Detection of hairline mandibular fractures become challenging due to lack of sharp discontinuity and presence of intensity inhomogeneity in a CT scan. Thus, there is always some chance of missing such a fracture at the time of manual checking.

Computer-aided fracture detection has gained popularity over the past decade. Some recent works in this area include use of texture for the detection of hip fractures by Yap *et al.* [2], detection of fractures in femur bones using combination of classifiers by Lum *et al.* [3], use of active contour modeling coupled with shape constraints for the detection of arm fractures by Jia and Jiang [4], femur fracture detection by divide-conquer approach in SVM's kernel-space by He *et. al.* [5] and use of Hough transform and gradient analysis for the detection of midshaft long-bone fractures by Donnelley *et. al.* [6]. Though the mandibular fractures are encountered frequently, there is a relative paucity of computer-aided detection of such fractures. Detection of well-displaced mandibular fractures (where the broken fragments suffer noticeable relative displacement, a sharp contrast with the present scenario) using Bayesian inference is reported in a work by Chowdhury *et al.* [7]. A MRF-based approach for hairline mandibular fractures can be found in another work by Chowdhury *et al.* [8]. However, the work described in [8] is computationally intensive. Furthermore, that work depends on an underlying assumption that bilateral symmetry is preserved in case of a mandible with hairline fracture, which may not necessarily hold in some cases.

In this paper, 2D slices containing fractured mandibles are separated first from the entire input sequence of broken craniofacial skeleton using Kolmogorov-Smirnov (KS) distance. In each 2D slice, a hairline fracture is modeled as a *cut* in the flow of intensities along the bone contours between two anatomical landmark points on the human mandible, called condyles. Geometry of the mandibular contours is exploited to build the flow network. In graph theory, this translates to finding a minimum cut in the flow graph between the *source* and the *sink*. A fracture is detected by determining a minimum cut using the max-flow min-cut algorithm of Ford and Fulkerson [9]. Unlike [8], the proposed method is computationally faster and does not require any such assumption as preservation of symmetry for mandibles with hairline fractures.

2. RETRIEVAL OF APPROPRIATE SLICES USING KOLMOGOROV-SMIRNOV DISTANCE

The input to our problem is a sequence of CT images showing fractured human craniofacial skeleton. Typically, a fractured mandible appears only in some slices within the entire sequence. An intensity-based image retrieval technique is applied with Kolmogorov-Smirnov (KS) distance as the measure of similarity and an unbroken mandible as the reference image to identify the fracture-containing 2D slices. Various distance measures had been applied for capturing the similarity in the content of two images in a content-based image-retrieval (CBIR) system [10]. A 2D slice of an unbroken mandible is treated as the reference slice. Each slice appearing in

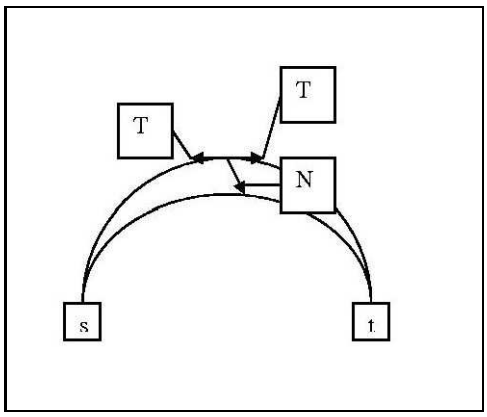

Fig. 1. A 2D flow network with a source s, a sink t and typical tangential (T) and normal (N) edges.

an input sequence is treated as a candidate slice. The histogram of the reference slice and each candidate slice are first computed. The respective histograms are modeled as probability distribution functions (pdfs), from which the cumulative distribution functions (cdfs) are then obtained. KS distance is used to find the similarity between the cdf of the reference slice and the cdf of each candidate slice. Let $X^c(x)$ and $Y^c(x)$ respectively denote the cdfs of the distributions $X(x)$ and $Y(x)$. Then, we can write the expression for the KS distance between these two cdfs as:

$$KS(X^c(x), Y^c(x)) = \sup_x |X^c(x) - Y^c(x)| \quad (1)$$

The candidate slices which yield a KS distance, smaller than that of a pre-determined threshold, are deemed as the ones containing the fractured mandible. An important advantage of using the KS distance is being a non-parametric distance measure, no particular form of distribution is necessary for its computation [11].

3. FRACTURE DETECTION USING MAX-FLOW MIN-CUT

In this section, we first discuss the construction of the flow network for a 2D CT slice with suitable choice of vertices, edges and capacity functions as edge weights. We will then justify our claim of correct mathematical modeling of the fracture detection problem as equivalent to identification of a minimum cut in the constructed flow network.

3.1. Construction of the flow network

In their formulation of flow network, Boykov and Jolly [12] choose all the pixels in an image as the vertices and establish edge connections amongst the 8 pixel neighbors. For the present problem, flow network $G = (V, E)$ is constructed in a different manner. It is noticed that a typical minor fracture appears at the bone contours. So, we choose the set of boundary pixels P on the two mandibular contours (i.e. the inner and the outer contour) as the vertices of the proposed flow network. The two condyles, which are anatomical landmark points at the two terminals of the jaw, serve as natural choices for the source vertex s and the sink vertex t. Thus, we can write: $V = P \cup \{s, t\}$.

We now explain how we have obtained all the mandibular contour points and the two condyles in a 2D slice. Some domain knowledge about the appearance of human mandibles in the CT scans is applied. Specifically, i) an intensity threshold for a mandibular pixel and ii) a bounding box for a mandible is assumed. Within the bounding box, we employ a boundary following algorithm [13] on pixels which satisfy the intensity threshold. Both the threshold value and the bounding box are kept constant for all the experimental datasets. The two condyles are two bottom-most points in the two halves of the image. So, we locate the condyles by finding two points on the mandibular contours with maximum value of the y-coordinate in the two halves of a 2D slice.

Since the boundary pixels for a mandible are essentially on an arc, we construct the *tangential* (T) and the *normal* (N) edges. For each boundary pixel on any particular mandibular contour, we create edge links with the immediate forward and backward neighboring pixels. These constitute the T edges. On the other hand, the N edges are established between any two normal (or near-normal) boundary points across the two contours q and r. In addition the first boundary pixel of both the contours (q_f, r_f) are attached to the source (s) and the last boundary pixel of both the contours (q_l, r_l) are attached to the sink (t). Therefore,

$$E = T \cup N \cup \{(q_f, s), (r_f, s), (q_l, t), (r_l, t)\}$$

The rationale behind having tangential and normal neighbors are guided by the geometry of the mandible as well as by the fracture pattern. A fracture appears along and also across the two mandibular contours (for example see figures (3) - (4)). The tangential edges are appropriate for capturing a fracture along the contour and the normal edges are suitable for identifying a fracture across the contour. So, by using both types of edges, a fracture is better modeled. Let j and k be any two consecutive points on one contour of a mandible with coordinates (x_j, y_j) and (x_k, y_k) respectively. Then the equation of the line that is normal to the contour at point j is given by:

$$(x_k - x_j)x + (y_k - y_j)y + (x_j(x_j - x_k) + y_j(y_j - y_k)) = 0 \quad (2)$$

In order to be a normal neighbor to the point j, a point on the other contour should ideally satisfy equation (2). However, it is not always possible to find the exact normal neighbor (primarily due to sampling error). So, we compute the distance d_{jm} of a set of competing candidate points m having coordinates (m_x, m_y) and choose the one which yields the minimum value of d_{jm}. From basic coordinate geometry, we can write:

$$d_{jm} = \frac{Am_x + Bm_y + C}{\sqrt{A^2 + B^2}} \quad (3)$$

where $A = (x_k - x_j)$, $B = (y_k - y_j)$ and $C = (x_j(x_j - x_k) + y_j(y_j - y_k))$. We choose a very simple capacity function as an edge weight between any pixel pair, with intensity and distance as the two parameters. Let I_p and I_q be the intensities of two pixels j and k and let d_{jk} be the Euclidean distance between them. Then the capacity function c_{jk} is given by:

$$c_{jk} = \frac{I_j I_k}{d_{jk}} \quad (4)$$

Since a typical fracture is marked by loss of bone, the intensity at a fracture site has a lower intensity than the surrounding bone. Additionally, the distance between two boundary pixels would be relatively higher if it encompasses a fracture site. This justifies the choice of the capacity function, (given by equation (4)) as both tangential and normal edges exhibit lower capacity at fracture sites. Very high capacity values were assigned to the edges which connect q_f and r_f to the source s and those which connect the sink t to q_l and r_l. By construction, all edges in our flow network have capacity > 0. Schematic diagram of a 2D flow network with source, sink, tangential and normal edges, is shown in figure(1).

3.2. Correctness of the Modeling

The purpose of this subsection is to provide an intuitive justification about the correctness of our modeling of fracture detection as a graph cut. We follow the framework of Boykov and Jolly [12]. From the discussion in the previous section, it is evident that every cut C on the flow network G satisfies following two properties:

1. C groups the vertices of G into two disjoint sets.
2. One set will contain the source s and the other set will contain the sink t.

The following theorem is essential to justify the correctness of our modeling.

Theorem. For any graph the maximum flow value from source s to sink t is equal to the minimal cut capacity of all cuts separating s and t. This is known as the Max-flow Min-Cut theorem [9].

Claim: A minimum cut C^* correctly identifies a fracture in our 2D flow network G.

Justification: The justification is based on the above Theorem and the construction of our graph with capacity function given by equation (4). We seek to determine the maximum flow between s and t. Using this Theorem, we obtain the minimum cut C^*. The minimum cut will consist of the cut edges in our flow network G. Basically, the cut edges are edges with comparatively low capacity values. From equation (4), it is evident that the low capacity edges are edges with relatively lower pixel intensity values and relatively higher distance values. These are exactly the characteristics of an edge in the vicinity of a fracture site. Note that since the broken fragments for a hairline fracture are not visibly out of alignment, a flow still continues between them with a drop in the value. This drop is due to the presence of the fracture, which is a bottleneck in the constructed flow network. Thus, identification of a minimum cut C^* corresponds to detection of a fracture in the 2D flow network G.

The computation of the augmenting path is done using a *breadth-first search*, as outlined in the *Edmonds-Karp* algorithm [14]. This implements the *Ford-Fulkerson* algorithm in worst case time $O(|V||E|^2)$, where $|V|$ denotes the cardinality of the vertex set V and $|E|$ denotes the cardinality of the edge set E in the flow network G.

4. EXPERIMENTAL RESULTS

Some results of KS distance-based image retrieval is shown in figure (2). In this figure, the two fracture containing slices out of a total of four are the ones which are similar in appearance to the unbroken reference slice and are hence retrieved. Note that the max-flow min-cut algorithm is applied exclusively to those slices which are being retrieved. We now show both qualitatively and quantitatively the performance of fracture detection using the 2D max flow-min cut algorithm. We have experimented with 43 different slices from 10 different data sets. Two different mandibles with identification of fracture sites are shown in figures (3) and (4) respectively. In each of these figures, the centers of the crosses mark the source (in the left half of the image) and the sink (in the right half of the image) vertices and the fractures are indicated by dark squares. From the execution of the max-flow min-cut algorithm, we obtain the edges in the cut set. Each such edge joins one vertex of the flow network on the *source*-side and another vertex of the flow network on the *sink*-side. For proper visualization, each such vertex is represented by black squares. It is evident from the figures that the fractures are identified accurately for both the cases. The ground-truth is obtained from the manually detections by experts. After comparing with the ground-truth, we find the fracture detection rate to be 79% and the false detection rate to be 41%.

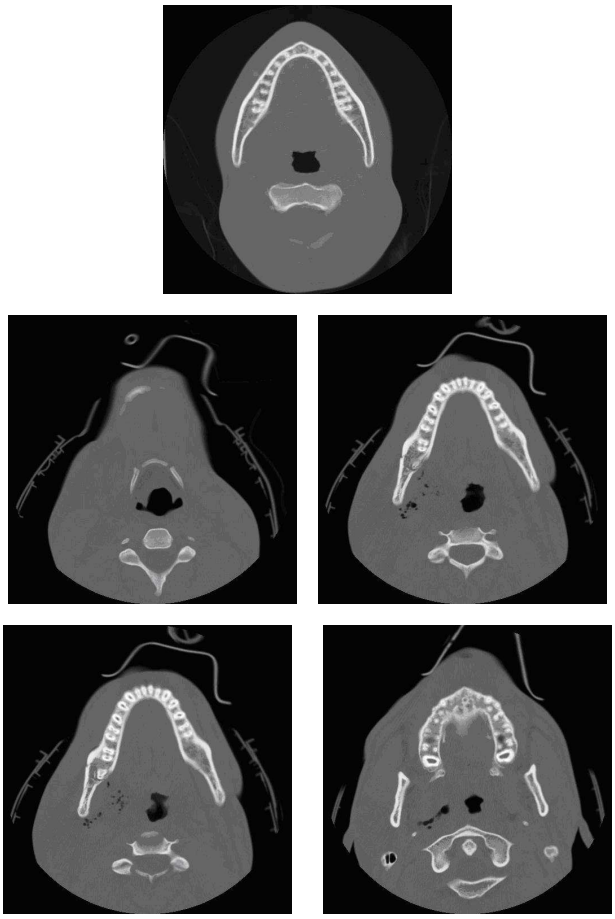

Fig. 2. Results from KS distance-based image retrieval for four slices from one sequence. Reference unbroken mandible in the first row. Right slice in the second row and the left slice in the third row are the ones retrieved.

5. CONCLUSION AND FUTURE SCOPE

In this paper, we model a hairline fracture as a minimum cut in an appropriately weighted flow network. The flow network is constructed based on the geometry of the human mandible and some prior knowledge of the fracture pattern. Simple capacity functions are designed as edge weights. Ford-Fulkerson algorithm is applied on the 2D flow networks to obtain a minimum cut. We obtain a fracture detection rate of 79% and a false detection rate of 41%. To the best of our knowledge, this is the first elaborate study of computer-aided detection of hairline mandibular fractures. Thus, though the detection results can be potentially improved, the present work with very little user intervention, serves as an important application for the radiologists and the craniofacial surgeons. From the computer vision perspective, the work has an elegant blending of nonparametric statistics, geometry and graph cut.

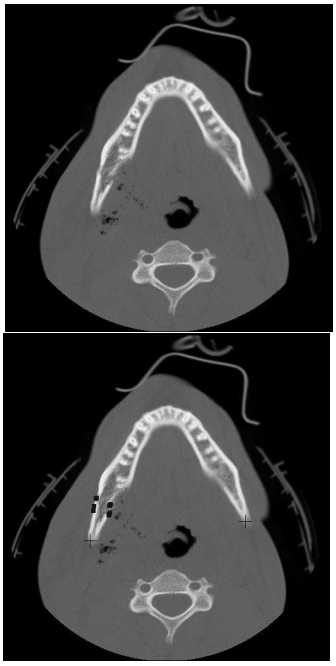

Fig. 3. 2D slice of a fractured mandible in the top. Fracture detection with source and sink identification in the bottom.

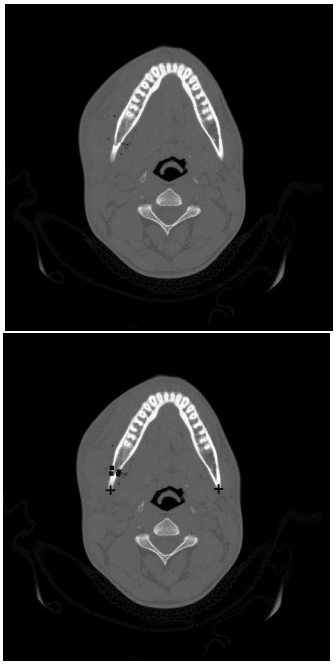

Fig. 4. 2D slice of a fractured mandible in the top. Fracture detection with source and sink identification in the bottom.

The future work would focus on increasing the fracture detection rate and reducing the false detection rate. This can be achieved by making the capacity function more robust with incorporation of anatomical knowledge. For example, we can use the information that tissue swelling and specific low intensity regions called emphysema [15] typically appear in the vicinity of a mandibular fracture.

6. REFERENCES

[1] J.M. Scianna R.E. King and G.J. Petruzzelli, "Mandible fracture patterns: a suburban trauma center experience," *Am. J. Otolaryngol.*, vol. 25, pp. 301–307, September-October 2004.

[2] W. K. Leow T. S. Howe D. W. H. Yap, Y. Chen and M. A. Png, ," in *Detecting Femur Fractures by Texture Analysis of Trabeculae*. IEEE Int. Conf. on Pattern Recognition (ICPR), 2004, pp. 730–733.

[3] Y. Chen T. Howe V. Lum, W. Leow and M. Png, ," in *Combining classifiers for bone fracture detection in X-ray images*. IEEE Int. Conf. on Image Processing (ICIP), 2005, pp. 1149–1152.

[4] Y Jia and Y Jiang, ," in *Active Contour Model with Shape Constraints for Bone Fracture Detection*. Int. Conf. on Computer Graphics, Imaging and Visualization (CGIV), 2006, pp. 90–95.

[5] W. K. Leow J. C. He and T.S. Howe, ," in *Hierarchical Classifiers for Detection of Fractures in X-Ray Images*. Int. Conf. on Computer Analysis of Images and Patterns(CAIP), 2007, vol. Springer LNCS 4673, W.G. Kropatsch, M. Kampel, and A. Hanbury (Eds.), pp. 962–969.

[6] G. Knowles M. Donnelley and T. Hearn, ," in *A CAD System for Long-Bone Segmentation and Fracture Detection*. IAPR Int. Conf. on Image and Signal Processing (ICISP), 2008, vol. Springer LNCS 5099, A. Elmoataz et al. (Eds.), pp. 153–162.

[7] G. Datta A.S. Chowdhury, S.M. Bhandarkar and J.C. Yu, ," in *Automated Detection of Stable Fracture Points In Computed Tomography Image Sequences*. IEEE Int. Symp. on Biomedical imaging (ISBI), 2006, pp. 1320–1323.

[8] S.M. Bhandarkar G.S. Datta J.C. Yu A.S. Chowdhury, A. Bhattacharya and R. Figueroa, ," in *Hairline Fracture Detection using MRF and Gibbs Sampling*. IEEE Int. Wkshp. on Applications of Computer Vision (WACV), 2007, p. p.56.

[9] Jr. L.R. Ford and D.R. Fulkerson, "Maximum flow through a network," *Canad. J. Math.*, vol. 8, pp. 399–404, 1956.

[10] J. Domingob M. Arevalillo-Herreza and F. J. Ferria, "Combining similarity measures in content-based image retrieval," *Pattern Recognition Lett.*, vol. 29 (16), pp. 2174–2181, September-October 2008.

[11] M. Hollander and D. A. Wolfe, ," in *Nonparametric Statistical Methods*. New York: Wiley, 1999.

[12] Y. Boykov and M.P. Jolly, ," in *Interactive Graph Cuts for Optimal Boundary & Region Segmentation of Objects in N-D Images*. IEEE Int. Conf. on Computer Vision (ICCV), 2001, pp. 105–112.

[13] R. Kasturi R. Jain and B. Schunk, ," in *Machine Vision*. McGraw Hill, NY, USA, 1995.

[14] R.L. Rivest T.H. Cormen, C.E. Leiserson and C. Stein, ," in *Introduction to Algorithms*. MIT Press, 2001.

[15] P. V. Giannoudis and H. Dinopoulos, "Current concepts of the inflammatory response after major trauma: an update," *Injury*, vol. 36(1), pp. 229–230, January 2005.